Title

Smartphone Operated Signal Transduction by Ion Nanogating (STING) Amplifier for Nanopore Sensors: Design and Analytical Application

Journal

ACS Sensors, 1(3)

ISSN

2379-3694

Authors

Özel, Rıfat Emrah
Kahnemouyi, Sina
Fan, Hsinwen
et al.

Publication Date

2016-03-25

DOI

10.1021/acssensors.5b00289

Peer reviewed

HHS Public Access

Author manuscript

ACS Sens. Author manuscript; available in PMC 2016 September 04.

Published in final edited form as:

ACS Sens. 2016 March 25; 1(3): 265–271. doi:10.1021/acssensors.5b00289.

Smartphone Operated Signal Transduction by Ion Nanogating (STING) Amplifier for Nanopore Sensors: Design and Analytical Application

Rıfat Emrah Özel[†,1,*], **Sina Kahnemouyi**[†,2], **Hsinwen Fan**[†,1], **Wai Han Mak**[1], **Akshar Lohith**[1], **Adam Seger**[1], **Mircea Teodorescu**[2], and **Nader Pourmand**[1]

[1]Biomolecular Engineering Department, University of California, Santa Cruz, Santa Cruz, CA 95064

[2]Computer Engineering Department, University of California, Santa Cruz, Santa Cruz, CA 95064

Abstract

In this report, we demonstrated a handheld wireless voltage-clamp amplifier for current measurement of nanopore sensors. This amplifier interfaces a sensing probe and connects wirelessly with a computer or smartphone for the required stimulus input, data processing and storage. To test the proposed Signal Transduction by Ion Nanogating (STING) wireless amplifier, in the current study the system was tested with a nano-pH sensor to measure pH of standard buffer solutions and the performance was compared against the commercial voltage-clamp amplifier. To our best knowledge, STING amplifier is the first miniaturized wireless voltage-clamp platform operated with a customized smart-phone application (app).

Keywords

Miniaturized sensing device; Voltage-clamp; Biosensor; Point-of-care; Nanopipette; Ionic Conductance; Low noise; Portable instrumentation

Over the past decade miniaturized sensing technologies such as biochips and microarrays have gained attention in biomedical diagnostics as an alternative to conventional laboratory assays. Conventional diagnostic methods require labor intensive sample treatment, very complex and large equipment and highly trained operators. More importantly, at present, diagnostic testing is expensive and must be performed remote from the patient-site, while low-cost, portable point-of-care devices are limited to a few assays[1]. These limitations are largely due to two reasons; (i) the difficulty in adapting assay protocols to a small-size, field-deployable sensor with little to no sample preparation, and (ii) the required sensitivity, temporal resolution and robustness of the signal transduction method.

[*]Corresponding author: ozelre@soe.ucsc.edu.
[†]These authors contributed equally.

Notes: The authors declare no competing financial interest.

Supporting Information: STING amplifier fabrication and engineering details. Details on the OpAmp used in the STING amplifier. SEM of nanopipettes. Detailed explanation of FTP and Bootup Process Appendix. The supporting information is available free of charge on the Internet at http://pubs.acs.org.

Integration of nanotechnology to existing sensing methods has resulted in the burgeoning development of nanoscale sensing tools. A new and attractive family of nanoscale sensors is nanopore sensors[2-4]. A nanopore sensor consists of a nanoscale opening (from 10 to 100 nm) at an insulator material. Our group has employed nanopipettes, quartz pipettes with a nanoscale pore at the tip, as nanopore sensing platform[5-8]. To fabricate versatile platforms, sensing probes can be tailored for various biological and non-biological recognition materials alone or in combination (*e.g.* enzymes, antibodies, ionophores, perm-selective membranes) to enhance the specificity and sensitivity[9]. Well-known electrochemical sensors applications include *in vivo* or *in vitro* detection of neurotransmitters, disease biomarkers, cell physiology, metal ions and DNA strands[10-12]. Nanopipette sensors enable the detection of biomolecules (e.g. cancer biomarkers, proteins, glucose) in a small amount of physiological sample as well as single-cell interrogation with high spatial resolution. Sensing with a nanopipette is based on the measurement of ion current passing through the nanopipette pore. The sensing is done by inserting an electrode into nanopipette and another in bath solution. An applied potential generates ion flow either to or from the nanopipette. Typically, alterations in the current signal due to ion flux or interaction of analyte molecules with the recognition materials immobilized at the tip, are at the order of low nanoamperes or picoamperes in magnitude. The acquisition of these weak current-signals requires low-noise electronics as amplifiers[13].

Indeed, improvement of the signal amplifier will be key to moving nanopore sensors into a commercially competitive point-of-use tool. In nanopore sensors, voltage-clamp amplifiers are typically used for current measurement. These amplifiers measure ionic conductance over time with two main techniques; (i) amperometric (current-readout at a fixed applied potential) and (ii) voltammetric (current-readout at specified potential window). Although commercially available voltage-clamp amplifiers (with their digitalizers) offer a low-level current detection circuit with high noise performance, they are physically oversized to conduct a point-of-care measurement, and require a computer to display the output signal and continuous power supply. Miniaturization of the amplifier while meeting necessary criteria, such as robustness, accuracy, reliability, ease-of-use and affordability is of great importance in the design novel nanopore sensors.

Here, we report the design, construction and characterization of a handheld, battery-operated, wireless voltage-clamp amplifier capable of connecting to either a computer or a smart phone through Wi-Fi. Since the current output is modulated with ionic conductance, we named the new platform “Signal Transduction by Ion NanoGating,” or STING amplifier. Figure 1A illustrates the high level hardware diagram of STING amplifier. Additionally, we tested the wireless STING amplifier with a nano-pH sensor to measure the pH of standard buffer solutions and compared the performance with a commercial voltage-clamp amplifier. To the best of our knowledge, STING amplifier is the first miniaturized wireless voltage-clamp platform operated with a customized smart-phone application (app).

Amplifier Design

The STING amplifier was designed with the types of signals typically associated with quartz nanopores used for protein, and chemical sensing. That is to say that it was optimized for

low noise and relatively low bandwidth (<1 kHz signals). Changes in the concentration of chemical species are expected to happen at a relatively slow timescale. The STING amplifier circuit was fabricated on a 13 × 13 cm^2, 4-layer printed circuit board (Figure 2). The total power consumption is 1070 mW. With a 9 V battery, the expected life is 5+ hours and there will be a red LED flashing if the battery is running out. Two on-board ID modules SW271 and SW272 give a unique ID of the board, allowing several boards working under same WiFi environment. Coding interface JP271 and JP273 allows several coding methods to program the microcontroller.

The signal amplification part of STING is the key component of the printed circuit board (PCB). With the reference electrode connected to ground and sensing electrode connected to the negative input the operational amplifier (OpAmp), this system can detect the current between these two electrodes at a given applied voltage (Figure 3A). The high sensitivity of the amplifier is of great importance for detection of minute amount of samples.

On the connected computers or portable devices, various functions of applied voltages can be created depending upon the measurement purposes. Those voltage functions are sent to a microcontroller on the STING amplifier. The microcontroller is programmed to receive the digital signals from the WiFi antenna, and then it sends the signals to a Digital-to-Analog Converter (DAC) as well as gathering digital signals from an Analog-to-Digital Converter (ADC) which will be transferred to the operating device. The DAC transfers the digital voltage signal to an analog voltage through the AD5662 chip, and then sends it through a 4 pole Bessel Low Pass Filter (LPF) with the cut-off frequency (-3 dB) at 2 kHz.

For sensing, the OpAmp 8627 is utilized to measure the current and to transfer the current signal to voltage signal. A detailed schematic is shown in Supporting Information (SI) Figure S-1. WL61 and WL62 are the detecting and reference probes, respectively. In the negative feedback OpAmp circuit, the OpAmp AD8627 amplifies the voltage difference between the two input nodes, 3 & 4. Here, node 3 of AD8627 is the positive input node signaling input from the user. The negative input node, node 4, and the output node are bound together to form a negative feedback circuit. Based on Kirchhoff's Current Law (KCL) and the assumption that no current flows into the negative input of the OpAmp and there is no bias between the negative and positive inputs of the OpAmp, we calculate the current goes through resistor “R61” as the current passing through the analyte solution, from the voltage value at node 5 of OpAmp. In an ideal scenario, the current applied to the solution, denoted as *I*, is calculated as follows:

$$I = \frac{V_{\text{node}5} - V_{\text{node}4}}{Z_{61}} \quad (1)$$

where Z_{61} is formulized as;

$$Z_{61}=\frac{R_{61}}{1+sR_{61}C_{61}} \quad (2)$$

Under the ideal OpAmp assumption, V_{node4} will not change. Therefore each node 5 voltage will represent a different current value, which means a different sample resistance under a given voltage. The total gain of AD8627 was limited to 50MΩ in order to preserve the stability of the system. Several precautions were implemented to prevent sensitivity to electromagnetic interference in the analog front end. These include using guard rings on the inputs, using a machined aluminum enclosure as the case for the amplifier, placing the WiFi components of the design physically far from the analog front end, and individually shielding the WiFi transmitters.

The voltage signal then goes to an accurate gain amplifier before the current-signal is analyzed. This accurate gain amplifier, LT1167, allows changes to the measurement range and resolution. The gain is controlled by resistors “R62”, “R63”and an internal resistance of 49.9kΩ and the gain G is given as;

$$G=\frac{49.9K\Omega}{R_{62}//R_{63}}+1 \quad (3)$$

The gain is set to 10 in order to keep the noise as low as possible while still allowing the transimpedance amplifier to operate without oscillating. Additionally, this stage serves to remove the bias introduced from the command voltage applied to the nanopore electrode.

The output of LT1167 goes through a low-pass filter (LPF) to minimize noise then to an ADC. The ADC circuit requires a differential input (-2.5 to +2.5 V) and it uses an ADS1271 24-bit wide band analog-to-digital converter chip (the resolution of the output signal will be 5×2^{-24}V). If the output of LT1167 is out of the -2.5V to +2.5V range, the ADC chip will overflow and give a constant maximum or minimum output. If this happens during a given experiment, the resistance of R_{62} and R_{63} can be changed to lower the gain of LT1167 but requires physical replacement of the resistors. The noise and drift from the ADC are insignificant compared to the noise generated by the rest of the system. At the final step, the ADC sends the signal back to the microcontroller, which communicates back to controller devices, such as computers and smart phones.

Software Design

The STING amplifier's software consists of two main components: (i) the firmware on the circuit board and (ii) the software on the user device (computer and portable device). For the current prototype, we chose WiFi as the mutual communication protocol. In addition, to ensure reliable delivery of the information on both ends, a higher level communication protocol was needed to transfer the information reliably. Therefore, we used the file transfer protocol (FTP) (based on the TCP/IP transfer communication protocol) to transfer the

stimulus and response data files between the two devices. The underlying TCP protocol in FTP connections insures the data delivery by retransmitting the data until the receiver sends an acknowledgement back indicating that the data is received. TCP packets also contain a checksum which is a small block of the packet with a unique value generated based on the raw data being transmitted. The checksum is then decoded in the receiver side to validate the authenticity of the data received and therefore provide the system with data integrity.

Both the stimulus and response files must then be encoded in the system in a language that is understandable by both devices. To insure the security and efficiency of the packets transferred between the client and the server, the measured data and the stimulus file are both respectively encoded in 24bit and 16bit special binary formats. These files are then converted to CSV/Excel files at each end for lab and home users to be able to easily view and edit them. CSV files are ASCII based files which require more space than binary files; however, with current high storage capacity of modern desktop computers and mobile devices using CSV files was a storage compromise worth making. In addition, our future implementations may add the option to save the data in other formats such as the Axon Binary Format (.abf) which can result in smaller file sizes. The current encoding and decoding techniques used for this communication are further described in more details in the supporting information, FTP Appendix.

Software design firmware

Designing the firmware for the STING amplifier involved three main parts: WiFi, FTP, and sensor. The STING amplifier firmware (i) programs the WiFi module as a WiFi hotspot, (ii) executes the initial handshake communication between the user device and the amplifier, and (iii) performs the following transmissions and packet receipts: (1) The biosensor behaves as an FTP client, accessing the FTP directory of the FTP server planted on the user's device. After the initial handshake has successfully finished, the amplifier FTP client becomes in charge of requesting to receive the stimulus file and sending the response file back. (2) The third part involves reading the sensory data from the digital ports. Before the sensory data enters the microcontroller, it is digitized by the ADC component to present the current measured by the STING sensor in binary. The microcontroller reads this data from its inputs and prepares it to be sent to the user.

In order to increase the security of packet transmission, in addition to specially formatting the data transferred in binary, the FTPS protocol was used. This protocol is an extension to FTP that adds Secure Socket Layer (SSL) and Transport Layer Security (TLS) support to the communication system. Newer systems are slowly more inclined to the use of HTTPS over FTP for file transfer which insures the same level of packet delivery guarantee with more complex security measures. However, HTTP requests include a set of headers which can be a significant amount of the transmitted packet when sending small amounts of data. On the other hand, FTP does not send such headers and keeps the actual data transmission to a minimum size. HTTP servers can be more easily deployed on client machines since it only requires an internet browser for accessing the files and sending commands to the server. Therefore, we plan to add HTTP support in our future implementations of this system to increase the ease of usability of the device on different platforms.

Figure 3B illustrates the FTP and WiFi relationship between the biosensor and the user device. The Firmware was programmed and debugged using the MPLAB®X IDE in the C programming language. All the code was then optimized for the on-board PIC32 microcontroller to efficiently handle the low available memory capacity and make use of just the right amount of processing power required for operating the STING amplifier.

Firmware contributes to battery saving

As the STING amplifier is designed for on-site measurements, and for conducting multiple measurements, the battery consumption must be minimal. Consequently two main battery-saving techniques were used to decrease the battery consumption: (1) Once the biosensor and client device are successfully connected, the Biosensor actively looks for data transmission for 70 seconds. If no measurement is conducted in that time window, the Biosensor activates the idle mode which halts the CPU on the microcontroller. In this mode, the system clock source continues to operate and enables some of the peripherals of our choosing to continue to perform. As a result, the external interrupts on the microcontroller can still detect the incoming wakeup signals from WiFi and resume the CPU as soon as a signal is received from the WiFi module. There is however a 100ms lead-time required for the CPU to wake from this state and start operating again. The power consumption of the microcontroller is directly related to the frequency of the active crystal oscillators. Therefore, when the CPU is halted, it consumes virtually no power. However, the primary oscillator keeps the peripherals active at a fraction of the maximum frequency which in our case was a ratio of 1:4. (2) In addition to the idle mode, the sleep mode is designed to turn off the Biosensor if it is not used for more than 5 minutes. In this case, the microcontroller will enter the sleep mode. The sleep mode, similar to the idle mode halts the CPU, but it also disables the main system clock, and a secondary lower power consuming oscillator is activated to enable select peripherals at a constant low frequency. Therefore, the CPU can still automatically start running after receiving an external wake up signal, but this process takes longer than in idle mode, because of the system clock being disabled.

Software Design: User Application/Program

Currently, the STING amplifier can be used on iOS devices, Apple OS X and Windows platforms. To provide the user with the maximum number of features, designing the software for each platform required platform-specific tools and techniques. However, all the programs and applications used on each platform exhibit the following mutual features: (1) Start a measurement wirelessly; (2) Options to generate various stimulus waves (sine, flat, triangular, *etc.*) including set frequency, set the total time of measurement and set amplitude; (3) Access to response data points; (4) Plot response data points; (5) Store the plots and response data points.

Client Software on Windows or Apple OS X platforms

Using the amplifier on a Windows or Apple OS X machine requires installing and configuring SFTP client software in addition to Microsoft Excel to view or modify the input and output data. FileZilla FTP Server on Windows and the native FTP server on Apple OS X can be configured to be used with the two specific ports utilized by the biosensor (2221, 2241). As soon as the FTP server is activated, the user and the biosensor are connected

through WiFi and the communication starts automatically. The stimulus and response files are both binary files with special encodings (described in the Appendix) to decrease the size of the transferred files between the client and the server and increase communication security. Since the mentioned files cannot be readily opened by spreadsheet programs like Excel, we have designed specific Excel files to encode and decode the binary response and stimulus files and convert them to and from easily editable spreadsheet files. Macros are embedded in these Excel files to give the user the comfort of converting the files in both directions by clicking on a single button. These Excel files give the user the option to generate their custom stimulus wave file as well as view the response data points from both channels to plot them.

Client Software Apple iOS platforms

The STING amplifier using the Apple iOS 8.1 and later for mobile devices enables users to control the measurements, store the data (as Excel or CSV files) and e-mail the plots or the data files (*e.g.* to collaborators or for further investigation on other devices). Additionally, the user could plot the results using the mobile application. Therefore, the iOS application was designed to be an independent, user-friendly tool to accommodate all the features the biosensor could provide.

Generating the Stimulus File and result collection

On all three platforms (iOS devices, Windows and Apple OS X) the biosensor application provides the user with the ability to construct the desired stimulus wave with a user friendly interface which lets the user choose the type of signal applied to the nanopipette electrode, in addition to its properties (waveform, start and end frequency, duration, and amplitude). Figure 1B displays the screenshot of the STING amplifier application on an iOS device. The application is designed to generate various stimulus signal wave with pre-set parameters. These parameters are then used to generate a digital wave in a 16bit binary format.

After the STING amplifier application ensures that the iOS device is connected to the biosensor hotspot, it activates its FTP server. The open source iOS-FTP-server library used to implement the FTP server then initiates the FTP communication, and manages the transfer of the encrypted files. Once the application makes sure that the measurement is successful, it stores the results as a CSV file and plots the data[5].

Noise Characterization of the STING amplifier

The STING amplifier is connected to the negative input of a resistive feedback amplifier with $V_n = 17.5\mathrm{nV}/\sqrt{\mathrm{Hz}}$, which is the prominent noise source (Figure 4C). The OpAmp AD8627 was chosen as it features low input-referred noise of $0.4\mathrm{fA}/\sqrt{\mathrm{Hz}}$ at 1kHz, low power consumption, and single supply operation in the range of 5V to 26V. The OpAmp has two inputs, “noninverting”(+) and “inverting” (-), and a single output. The OpAmp converts the input current signal in the solution into a voltage signal in the output. The output potential flows through feedback capacitor C_F and resistor R_F resulting in a potential at the inverting input, which is equal to the potential difference between the solution and the counter electrode. The feedback capacitor has a capacitance of C_F = 4.7 pF while the resistor

has a resistance of 49.9MΩ. The total output noise power-spectral density is calculated based on the equation (4);

$$I_{\mathrm{out,tot}} = \sqrt{I_{\mathrm{in,tot}}^2} \cdot \sqrt{B} \cdot G \quad (4)$$

where B is the bandwidth, G is the gain of the negative feedback amplifier, and $\sqrt{I_{\mathrm{in,tot}}^2}$ is the input noise power density given by with the equation (5).

$$\sqrt{I_{\mathrm{in,tot}}^2} = \sqrt{I_s^2 + I_{n,\mathrm{op}}^2 + I_{\mathrm{RF}}^2} = \sqrt{I_s^2 + \frac{V_{\mathrm{in,tot}}^2}{\mathrm{RF}^2} + \frac{4kT}{\mathrm{RF}})} \quad (5)$$

I_s is the noise of sensor impedance, $I_{n,op}$ represents the op-amp input current noise, and I_{RF} refers to feedback resistor (R_F) noise. k is the Boltzmann constant and T the temperature in Kelvin. Performing a noise analysis using LTspice circuit analyzer, the input referred noise is predicted to be 0.73 pA_{RMS}.

The noise characterization of the wireless amplifier compares closely to the MultiClamp 700B Microelectrode (Molecular Devices), without the additional bulk and expense (Figure 4A and B). Recently many efforts have been given to the development of low noise circuit designs to replace the patchclamp, which is broadly used for bioinformatics studies[14, 15]. In this noise measurement, a Digidata 1322A is connected to the MultiClamp 700B to digitize the output current with Clampex 9 software. An open circuit headstage is connected to the MultiClamp 700B. The wireless amplifier is powered by a 9V- charger and zero voltage is applied. The headstage and the wireless circuit board are kept in an open environment during the noise measurements. The noise is measured over a bandwidth of 2000 Hz, 4-pole Bessel filter and total gain of 500 MΩ. The noise of the wireless amplifier was equal to the 700 B at 1.4 pA_{RMS}. This compares well to the predicted value of 0.73 pA_{RMS}. The difference between measured and calculated values could be due to noise pickup from the environment, or the exclusion of the digital-to-analog and analog-to-digital circuitry from the noise calculations.

Analytical Performance of the STING amplifier

To demonstrate the analytical performance of the STING amplifier and to compare it versus the gold standard patch-clamp device, MultiClamp 700B[16], we measured the pH of the standard pH solution with a chitosan-modified quartz nanopipette. Recently, we developed and characterized this nano-pH sensor for the measurement of intracellular pH at single-cell level. Representative scanning electron microscope (SEM) images of the nano-pH probe are shown in Figure S-2. An Ag/AgCl wire was placed, as working electrode, into the nanopipette filled with 10 mM PBS (pH 7.0). The pH measurements were conducted with a linear voltage sweep between -0.5 and 0.5 V *vs.* pseudo Ag/AgCl reference/counter electrode. The pH solutions tested were 0.1 mM PBS adjusted by 1 M NaOH or HCl. The

experimental parameters for both the STING amplifier and MultiClamp 700B were identical with a bandwidth of 2000 Hz. The sensing parameters at which the nano-pH probes were optimized were 0.1 V/sec and 5 ms, voltammetric scan rate and sampling rate, respectively.

The purpose of fabricating the STING amplifier was to engineer an analytical instrument that enables on-site measurements in biological samples, and reduces the need for conventional clinical devices. Figure 5 compares the pH measurements carried out with the STING amplifier and a MultiClamp 700B. Current traces obtained with the STING amplifier for base (Figure 5A) and acid (Figure 5C) correlated well with the ones obtained with MultiClamp (Figure 5B and D). For the acidic pH measurement, the current-response variation at 0.5 V between the STING amplifier and MultiClamp 700B was 12.6 (± 9.4) %, while the basic pH measurement variation was 10.46 (± 7.0) %. Variations observed are consistent with variability and drift observed with quartz nanopipettes.

Conclusions

Current developments in printed circuit board technology allow the fabrication of miniaturized, low-noise, low-power and, more importantly, portable wireless analytical instrumentation for clinical assays. Miniaturized devices can substitute for their benchtop counterparts at remote patient sites. The STING amplifier reported herein is a portable dual-channel patch-clamp analyzer. The circuit board construction and software design, which are discussed in detail, have general applicability in the nano-sensor field. The noise characterization demonstrates that the STING amplifier has an instrumental noise as low as 0.73 pA_{RMS} which compares well with MultiClamp 700B, the commercial equivalent. Additionally, we have performed an *in vitro* pH measurement with the STING amplifier and compared it with the commercial patch-clamp amplifier. Results suggest that the STING amplifier can be used as a cost-effective alternative to its expensive commercial counterparts. Furthermore, we have written an iOS application which eliminates the need for a computer to operate the STING amplifier. The STING amplifier described here will be further improved by adding more channels and remodeling the circuit board for a smaller profile. Bluetooth wireless communication will be implemented to reduce power consumption and to pair the new amplifier with portable devices. Additionally, a set of new techniques, including amperometry, differential pulse and square wave voltammetry, will be enabled for the users to increase the spectrum of application of the STING amplifier.

Supplementary Material

Refer to Web version on PubMed Central for supplementary material.

Acknowledgments

This work was supported in part by grants from the National Institutes of Health [P01-35HG000205[, and National Institute of Neurological Disorders and Stroke [R21NS082927[. We acknowledge Dr. Tom Yuzvinsky for image acquisition and the W.M. Keck Center for Nanoscale Optofluidics for use of the FEI Quanta 3D Dualbeam microscope.

References

1. Giljohann DA, Mirkin CA. Drivers of biodiagnostic development. Nature. 2009; 462:461–464. [PubMed: 19940916]
2. Umehara S, Karhanek M, Davis RW, Pourmand N. Label-free biosensing with functionalized nanopipette probes. Proc Natl Acad Sci U S A. 2009; 106:4611–4616. [PubMed: 19264962]
3. Kang EJ, Takami T, Deng XL, Son JW, Kawai T, Park BH. Improved Ion-Selective Detection Method Using Nanopipette with Poly(vinyl chloride)-Based Membrane. J Phys Chem B. 2014; 118:5130–5134. [PubMed: 24766420]
4. Plesa C, Ruitenberg JW, Witteveen MJ, Dekker C. Detection of Individual Proteins Bound along DNA Using Solid-State Nanopores. Nano Lett. 2015; 15:3153–3158. [PubMed: 25928590]
5. Actis P, Rogers A, Nivala J, Vilozny B, Actis P, Jejelowo O, Pourmand N. Reversible thrombin detection by aptamer functionalized STING sensors. Biosens Bioelectron. 2011; 26:4503–4507. [PubMed: 21636261]
6. Actis P, Mak A, Pourmand N. Functionalized nanopipettes: toward label-free, single cell biosensors. Bioanal Rev. 2010; 1:177–185. [PubMed: 20730113]
7. Vilozny B, Actis P, Seger RA, Vallmajo-Martin Q, Pourmand N. Reversible cation response with a protein-modified nanopipette. Anal Chem. 2011; 83:6121–26. [PubMed: 21761859]
8. Ozel RE, Lohith A, Mak WH, Pourmand N. Single-cell intracellular nano-pH probes. RSC Adv. 2015; 5:52436–52443.
9. Wang J. Sol–gel materials for electrochemical biosensors. Anal Chim Acta. 1999; 399:21–27.
10. Özel RE, Hayat A, Andreescu S. Recent Developments in Electrochemical Sensors for the Detection of Neurotransmitters for Applications in Biomedicine. Anal Lett. 2015; 48:1044–1069. [PubMed: 26973348]
11. Ley C, Holtmann D, Mangold KM, Schrader J. Immobilization of histidine-tagged proteins on electrodes. Colloids Surf, B. 2011; 88:539–551.
12. Sassolas A, Blum LJ, Leca-Bouvier BD. Immobilization strategies to develop enzymatic biosensors. Biotechnol Adv. 2012; 30:489–511. [PubMed: 21951558]
13. Goldstein B, Dongsoo K, Jian X, Vanderlick TK, Culurciello E. CMOS Low Current Measurement System for Biomedical Applications. Biomedical Circuits and Systems, IEEE Trans. 2012; 6:111–119.
14. Rosenstein JK, Wanunu M, Merchant CA, Drndic M, Shepard KL. Integrated nanopore sensing platform with sub-microsecond temporal resolution. Nat Meth. 2012; 9:487–492.
15. Crescentini M, Bennati M, Carminati M, Tartagni M. Noise Limits of CMOS Current Interfaces for Biosensors: A Review. IEEE Trans Biomed Eng. 2014; 8:278–292.
16. Falconer M, Smith F, Surah-Narwal S, Congrave G, Liu Z, Hayter P, Ciaramella G, Keighley W, Haddock P, Waldron G, Sewing A. High-Throughput Screening for Ion Channel Modulators. J Biomol Screen. 2002; 7:460–465. [PubMed: 14599362]

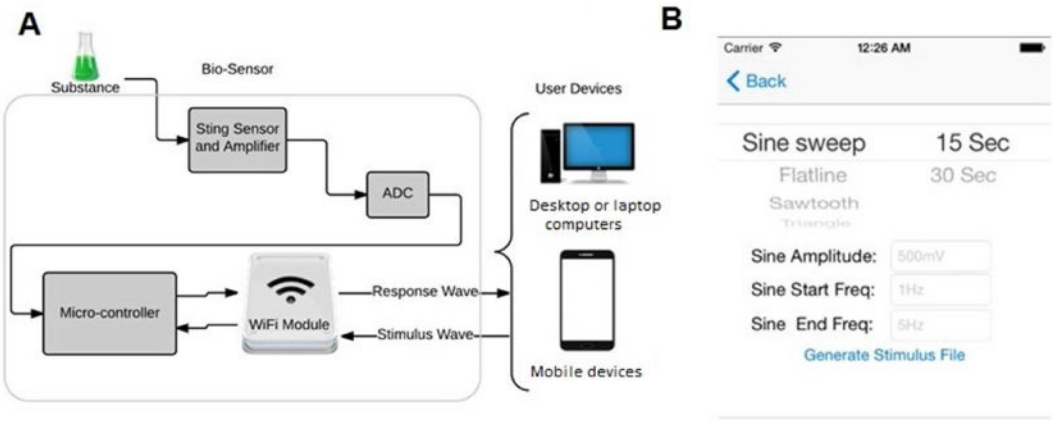

Figure 1.

(A) Schematic of high level of STING amplifier diagram. The STING amplifier has two channels enabling two individual measurements simultaneously. **(B)** Screenshot of the STING amplifier application on an iOS device. The application is designed to generate various stimulus signal wave with pre-set parameters.

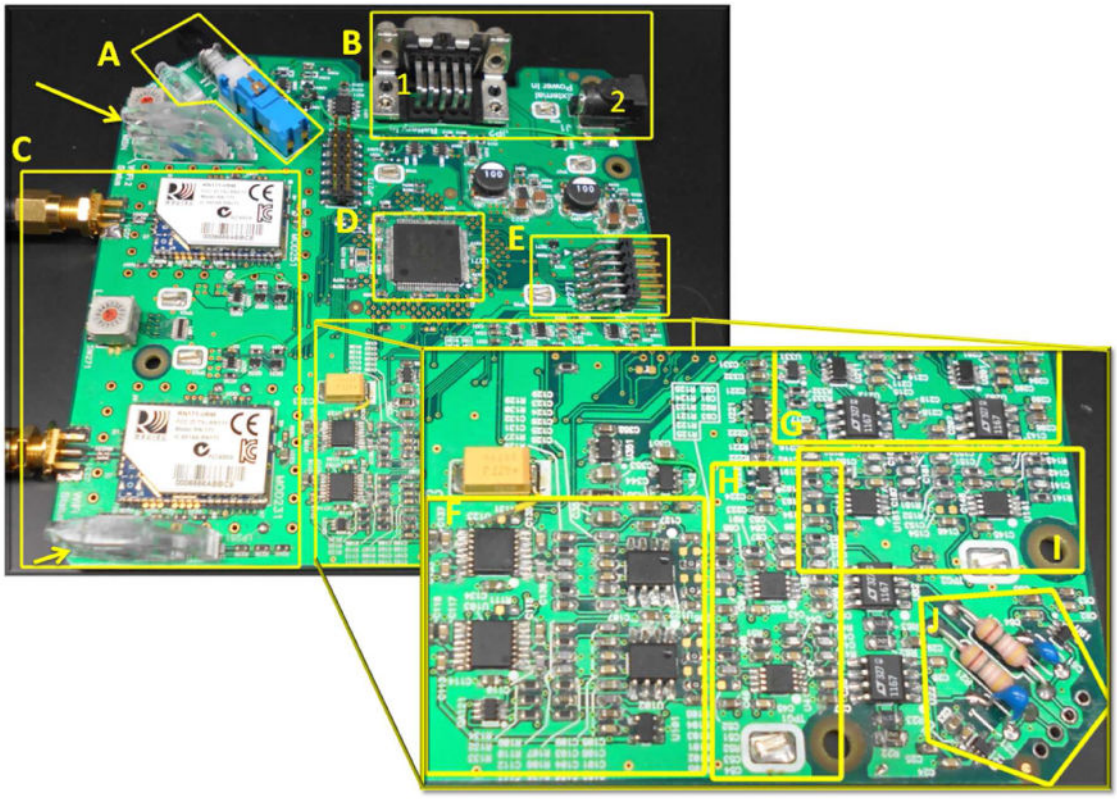

Figure 2.

Photo of the STING amplifier printed circuit board. Individual functional parts are grouped in yellow boxes. **(A)** Power switch and LED indicator. **(B)** Source power input by 9V battery connection (1) or wall power adapter (2). **(C)** WiFi communication modules with status indicator LEDs (arrows). **(D)** Microcontroller PIC32 processor. **(E)** Onboard coding interface for Firmware updates. **(F)** Analogue-Digital-Converter (ADC) circuit. **(G)** Digital-Analogue-Converter (DAC) circuit. **(H-I)** Low-pass filter circuits for each channel. **(J)** Two channel sensor connection. Each channel has a working and counter/reference connection.

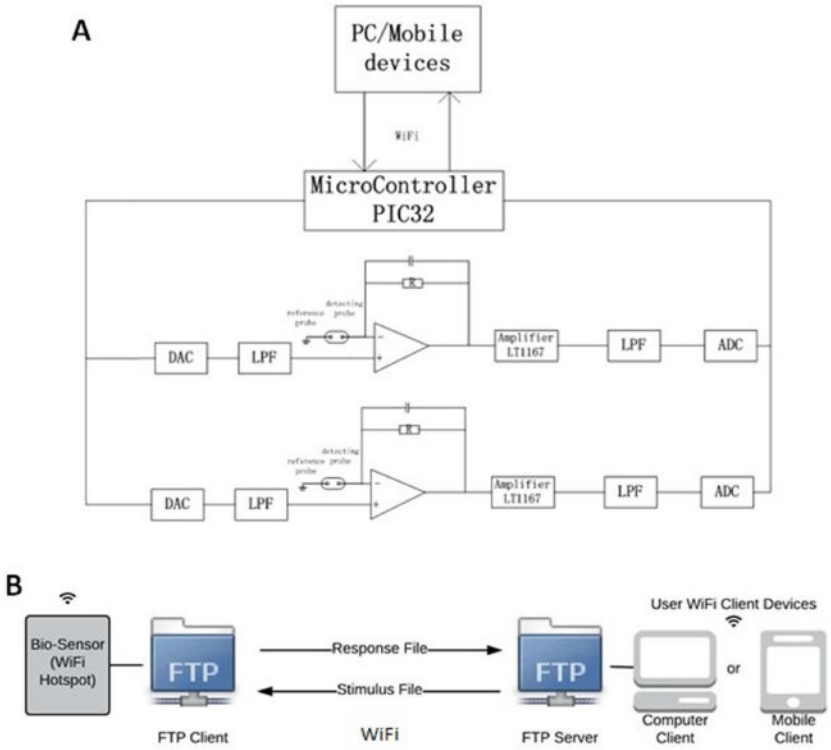

Figure 3.

(A) Block diagram of the STING amplifier. The amplifier has two parallel channels that can be operated individually or together. DAC: Digital-to-analogue converter; LPF: Low-pass filters; ADC: Analogue-to-digital converter; R: Resistance. **(B)** Schematic of the FTP and WiFi relationship between STING amplifier and controller device.

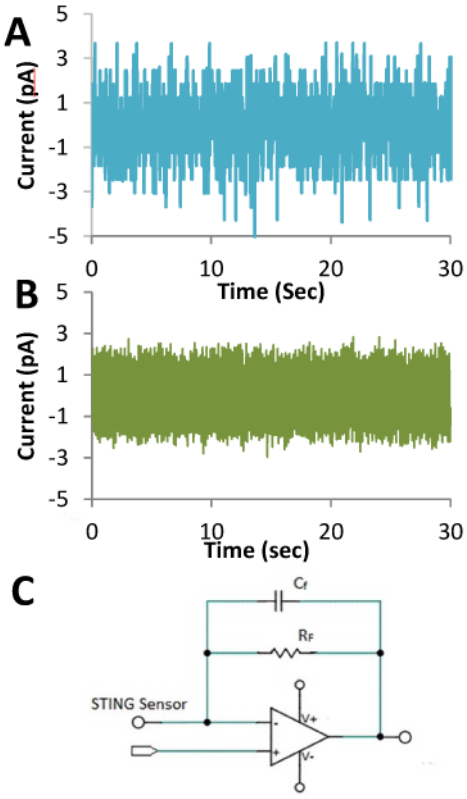

Figure 4.

Instrumental current noise comparison of **(A)** MultiClamp 700B *vs.* **(B)** STING amplifier. **(C)** Simplified block diagram of the sensing part of STING amplifier.

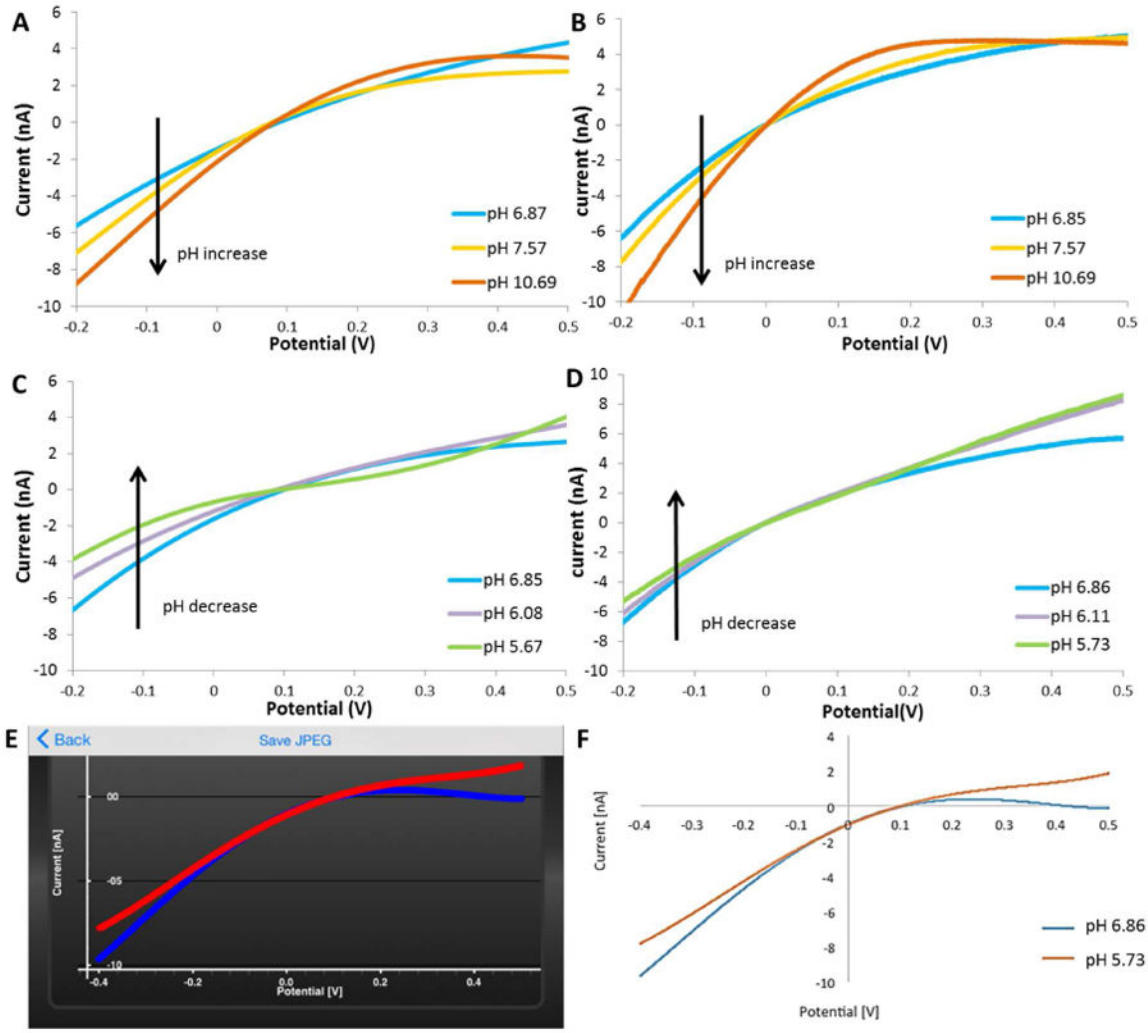

Figure 5.

Representative linear sweep voltammetric signals for pH measurements with nano-pH sensor obtained employing the STING amplifier (**A** and **C**) and MultiClamp 700B (**B** and **D**). 10 mM PBS was used as nanopipette filling solution. Acid and base titration experiments were conducted with the same nanoprobes respectively. Similar current-responses were recorded with the STING amplifier and the reference system. All supporting electrolytes were 0.1 M PBS with various pH levels adjusted with 1 M HCl or NaOH. Acid titrations were performed with the same pH nanosensor using **(E)** STING smartphone app and **(F)** computer controller.